A triple-GEM detector with pad readout for high rate charged particle triggering

G. Bencivenni [a] G. Felici [a] F. Murtas [a] P. Valente [a]
W. Bonivento [b,*,1] A. Cardini [b] A. Lai [b] D. Pinci [b,c] B. Saitta [b,c,1]
C. Bosio [d]

[a] *Laboratori Nazionali di Frascati - INFN, Frascati, Italy*
[b] *Sezione INFN di Cagliari, Cagliari, Italy*
[c] *Università degli Studi di Cagliari, Cagliari, Italy*
[d] *Sezione INFN di Roma, Roma, Italy*

Abstract

In this paper results of a time performance study of triple-GEM detectors are discussed.

This study was driven by an R&D activity on detectors for the Level 0 LHCb muon trigger. However, the results presented in this paper are of more general interest, i.e. for experiments with high rate charged particle triggering.

Little interest was given so far to time performance of GEM detectors. Only one group measured double-gem detector time resolution with the Ar/CO_2 (70/30) gas mixture.

Our study aimed at triple-GEM detector optimisation for good time performance through a detailed investigation of the role played by detector geometry, electric fields and gas mixture.

The results reported here, in particular when using the gas mixture $Ar/CO_2/CF_4$ (60/20/20), considerably improve the time performance discussed in the above mentioned paper and make the triple-GEM detector a promising option for high rate charged particle triggering.

Key words: GEM, tracking
PACS: 29.40.Cs, 29.40.Gx

* Corresponding author
Email address: walter.bonivento@cern.ch (W. Bonivento).
[1] Now at CERN

1 Introduction

Detectors with one or more GEM foils [1] have been extensively studied in the last four years and are currently used as tracking device [2] or as a part of a tracking device [3] in high rate experiments. In particular, when space resolution in the range 50 μm to few mm is required, they represent a cheaper solution compared to the well established solid state detector technique, being also quite robust against radiation damage.
However, little interest was devoted so far to the optimisation of the time response of GEM detectors.
One important application of tracking detectors is triggering. In a collider environment a critical issue is bunch crossing identification, which sets an upper limit to the detector time resolution, when requiring high trigger efficiency.
The work described in this paper originated from an R&D activity on detectors for the Level 0 LHCb muon trigger. For the LHC collider, the time between bunches is 25 ns.
Only one paper [4] has so far presented a measurement of a double-GEM detector time resolution, with the gas mixture Ar/CO_2 (70/30). The authors of that paper quote a resolution of about 10 ns r.m.s. without software corrections (though they argue that a relevant contribution to the resolution comes in their experiment from the limited rise-time of the electronics).
In this paper we present a detailed study of a triple-GEM detector optimisation for good time performance, through a detailed investigation of the role played by detector geometry and electric fields. A new gas mixture with the CF_4 gas, which we consider better from timing point of view, was also studied and results are presented here. High rate performance, ageing and discharge rate studies with the optimised detector configuration will be the subject of a future publication.
Section 2 briefly describes the main properties of the triple-GEM detector. In section 3 the requirements for a high rate detector for muon triggering in LHCb are presented and compared to known properties of GEM detectors. In section 4 detector optimisation for high rate charged particle triggering is discussed and in section 5 effective gain and beam test measurements are described.

2 The triple-GEM detector

A GEM is made by a thin (50 μm) kapton foil, copper clad on each side, perforated with high surface density of holes, each one acting as an electron multiplication channel. Each hole has a bi-conical structure with external (internal) diameter of 70 μm (50 μm) and a pitch of 140 μm. The bi-conical shape of the hole minimises the effect of charging-up of the kapton inside the

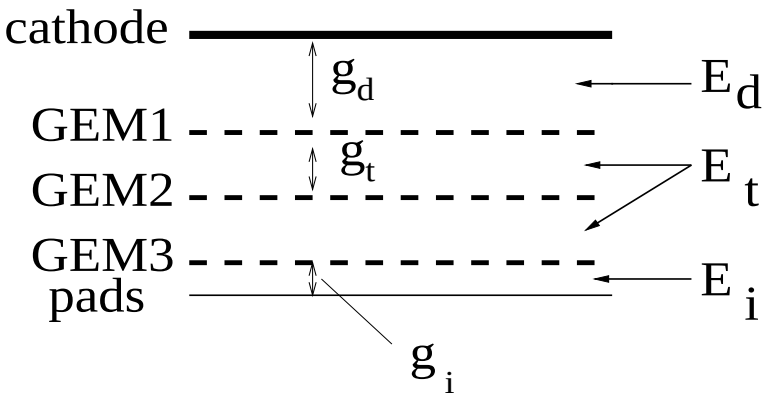

Fig. 1. Cross-section of the triple-GEM detector. E_d, E_t and E_i are the drift, transfer and induction fields, respectively; g_d, g_d, and g_i are the drift, transfer and induction gaps, respectively.

holes and is a consequence of the double mask process used in standard photolitographic technologies.
A typical voltage difference of 350 to 500 V is applied between the two copper sides, giving fields as high as 100 kV/cm into the holes, resulting in an electron multiplication up to a few thousands.
Multiple structures realized by assembling two or more GEMs at close distance allow high gains to be reached while minimising the discharge probability.
The triple-GEM detector, which consists of three gas electron multiplier (GEM) foils sandwiched between two conductive planes, one of which, the anode, is segmented in pads and connected to the readout electronics, can be effectively used as tracking detector, with good time and position resolution performances.
A cross-section of this detector, together with the labelling of the different detector parameters used in this paper, is shown in Figure 1.
The ionisation electrons, produced in the gap between the cathode and the first GEM foil (drift gap) by the charged particles crossing the GEM, are attracted by electric fields through the three GEM foils where they get multiplied. Once they cross the last GEM foil they drift to the anode in the so called induction gap, giving rise to an induced current signal on the pads.

3 Detector requirements

The LHCb muon detector system consists of 5 stations of chambers. The first station (M1) is located in front of the electromagnetic calorimeter while the other four (M2 to M5) are located behind the calorimeters and are separated one from the other by iron walls [5].
The main purpose of the muon system is to give the Level 0 trigger for muons coming from b-flavoured hadron decays. To do this, the trigger requires for a muon candidate to fire all five stations with unambiguous bunch-crossing

identification with an efficiency of 95% for the muons inside the acceptance.
Most of the muon system will be equipped with Multi-Wire Proportional-Chambers (MWPC), while the outer part of stations 4 and 5 will be equipped with Resistive Plate Chambers (RPC).
No technology has been chosen yet for the inner part of station 1, where particle rates above 100 kHz/cm^2 are expected. The surface covered by these chambers is 2.9 m^2 per layer.
A detector located in region 1 and 2 should satisfy very tough requirements, in terms of rate capability, efficiency, dead time, number of adjacent pads fired per track and radiation hardness.
To achieve 95% overall trigger efficiency on muons in a bunch crossing interval, each station must have an efficiency of more that 99%. For redundancy, two independent detector layers per station are foreseen, which will be logically OR-ed; therefore, the requirement for the single chamber is of at least 95% efficiency.
MWPC and RPC detectors already selected for LHCb already satisfy the efficiency requirement with a leading-edge time pick-off method. For uniformity of the readout chain, this method should also be used for the inner regions of M1. In any case, the high charged particle flux expected in the detector would anyway disfavour time pick-off methods lengthening the pulse shape such as zero-crossing or constant-fraction, since they would increase inefficiency by dead time. Moreover, as will be discussed in section 4, an important contribution to time resolution in GEM detectors is primary cluster distribution. Therefore, one expects little gain from methods which are meant to compensate for gain fluctuations. It is however fair to say that a detailed study of this issue was not performed.
The detector will be operated up to a rate of 460 kHz/cm^2; correct detector response of a triple-GEM detector operated at similar high flux of charged particles was already verified [4].
To optimise transverse momentum resolution of 20 %, the pad multiplicity, i.e. the number of adjacent detector pads fired when a track crosses the detector, should not exceed the value obtained from geometrical considerations of detector crossing angle in the experiment, i.e. should not be larger than 1.2 for a 10x25 mm^2 pad size. Published results indicate a transverse avalanche size in GEM detectors of about a mm [4].
Dead time should be less than 50 ns; this puts stringent limits on both pulse width and on the maximum tolerable discharge rate. Discharge probabilities for triple-GEM detectors were already measured both with α sources [6] and charged particle beams [2]. However, the discharge probability strongly depends on detector parameters and gas mixture and measurements will have to be performed with the final chosen configuration.
The detector should also operate in a harsh radiation environment. If it is operated with the Ar/CO_2 (70/30) gas mixture and a total gain of 10^4, it would integrate a charge of about 6 C/cm^2. Ageing measurements were so far performed only on double-GEM devices with the Ar/CO_2 (70/30) gas mixture [7];

no degradation of the response was observed up to 70 mC/cm^2.

4 Detector optimisation for high rate triggering operation

Signal formation in GEM detectors takes place in the induction gap, which behaves in this respect as an ionisation chamber.
Assuming no cross-talk to adjacent pads, the signal induced on a pad by one electron drifting in the induction gap for a time $t_{drift} = g_i/v_{drift}$, where v_{drift} is the drift velocity of electrons and g_i is the induction gap size, is a current pulse of intensity $I = e/t_{drift}$ and duration t_{drift}.
The total signal induced on a pad by a track crossing the GEM is given by the sum of signals due to the single ionisation electrons, amplified by the multiplication through the GEM foils, each one delayed in time by the corresponding electron drift time in the drift gap. The total signal has then to be convoluted with the amplifier response to get the signal at the discriminator input. For leading edge triggering, which is considered in this paper, the discriminator crossing on the signal rising edge gives the time of the event.
The signal rising edge at the amplifier input has a stepwise profile, each step corresponding to the signal of an ionisation cluster (the time spread of electrons within a ionisation cluster is much smaller than the time difference between clusters). The detector time resolution is determined by the time distribution of these clusters and the corresponding signal amplitude fluctuations, both in the ionisation process and in the multiplication through the GEMs.
For the measurements discussed in this paper, very fast (peaking time less than 10 ns) and low noise (equivalent noise charge less than 1500 e^-) amplifiers, already developed for wire chamber operation, were used. Therefore no optimisation of the signal processing chain was performed.
The number of ionisation clusters produced in the drift gap follows a Poisson distribution. Therefore, the distance x of the ionisation cluster nearest to the first GEM has the probability distribution $P(x) = n \cdot exp(-nx)$, with $\sigma(x) = 1/n$, where n is the average number of ionisation clusters per unit length and $\sigma(t) = 1/(n \cdot v_{drift})$ [8]. The other ionisation clusters have a probability distribution with larger $\sigma(t)$, though still proportional to $1/(n \cdot v_{drift})$. Thus, in order to optimise the time performance of the detector, a large average atomic number and high drift velocity gas mixture should be used [8].
Two gas mixtures were used in the measurements reported in this note: Ar/CO_2 (70/30), which we used as reference for it was studied in the past, and $Ar/CO_2/CF_4$ (60/20/20), which we consider to have better time characteristics for the GEM detector. Among the fast and high average atomic number gases, tetrafluoromethane (CF_4) is the most frequently used because it is non-flammable, non-corrosive, non-toxic, and shows a good compatibility

with most of metals, plastics and resins used in gaseous detectors construction.
The drift velocity for the two mixtures [9,10] is shown in Figure 2. The $Ar/CO_2/CF_4$ (60/20/20) mixture has 25% higher drift velocity at 3 kV/cm than the Ar/CO_2 (70/30) one. The number of ionisation clusters per cm for the two mixtures is predicted to be 45.5 and 34.3, respectively [11]. Thus, from primary cluster distribution and drift velocity one expects the r.m.s. of the time distribution to improve with the ternary mixture by about 50%.
To improve the detection efficiency and reduce the influence of the time-walk

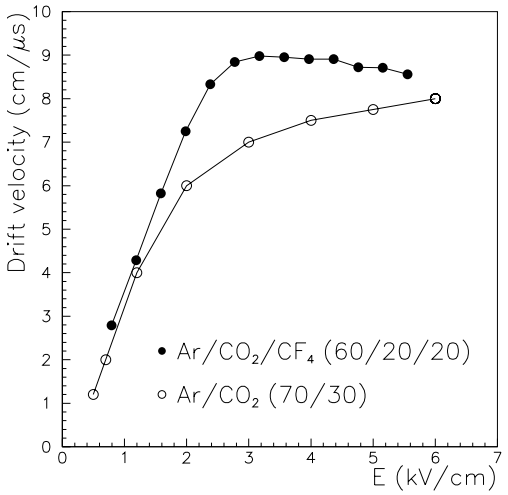

Fig. 2. Electron drift velocity for $Ar/CO_2/CF_4$ (60/20/20) and Ar/CO_2 (70/30).

effect it is also useful to have large amplification in the gas and therefore a high total GEM gain.
A measurement of the effective gain, i.e. the combined effect of electron multiplication and transparency through the GEMs, for the two gas mixtures was performed with an X-ray tube as a function of the sum of the three GEM voltages (with the assumption, always verified in the past, that GEM detector gain depends only on the sum of voltages) and will be presented in section 5.3.
To achieve a given total gain, instead of raising the three GEM voltages at the same time, we considered better for the time performance to have a higher voltage U_{gem1} on the first GEM. In this way the effect of gain fluctuations on the ionisation electrons on total pulse height is reduced. Moreover, the influence of the *bi-gem* effect, i.e. the amplification of the ionisation electrons produced in the first transfer gap, out of time with respect to those coming from the drift gap by $\Delta t = g_t/v_{drift}$, where g_t is the transfer gap size, is also reduced. This choice is also good from the point of view of discharge probability since previous studies [6] indicate that discharge probability depends both on total gain and on voltage of the last GEM.
Detector gap sizes and field values optimisation for time performance is the result of a compromise among some conflicting requirements.

The size of the drift gap g_d has to be large enough to minimise inefficiencies in charged particle detection but should be kept small to reduce the dead time due to pulse width. With a 3 mm gap and fast amplifiers, the pulse width should be less than 40-50 nsec, which satisfies the requirements.
Since the longitudinal diffusion is minimal due to the small drift path of the electrons in the detector, the main effect of the transfer gap is to give a delay to the detected pulse. However, to minimise the impact of the above mentioned *bi-gem* effect, the size of the transfer gap g_t was kept to 2 mm.
Given the fast amplifiers we used in this test, the size of the induction gap g_i should be small to increase the amount of charge integrated by the amplifier (with a large integration time constant the gap size would not matter) and to reduce the cross-talk fraction, by both direct induction and capacitive coupling. A lower limit to the size of the induction gap was considered to be between 1 and 1.5 mm, to minimise the discharge probability, which is likely to be affected by the gap size itself [6].
The best values for E_d, the field in the drift gap, E_t, the field in the transfer gaps and U_{gem1} were experimentally determined by optimising the detector efficiency in a given time window. The value of E_i, the field in the induction gap, was held during these measurements at 5 kV/cm.

5 Experimental measurements

5.1 Detector construction

For the tests described in this paper, two similar detector prototypes, one built by INFN Cagliari and one built by INFN Frascati, which will be labelled A and B in the following, were used.
The three 10×10 cm^2 active surface GEM foils [15] were fixed on G10 frames

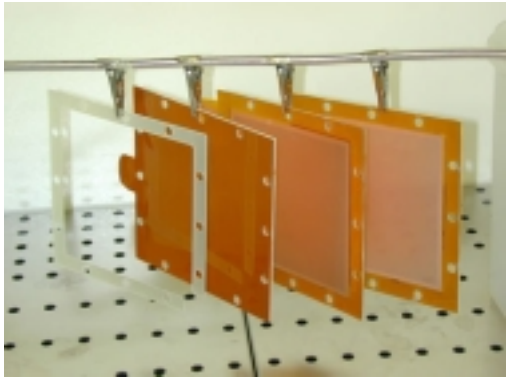

Fig. 3. The three GEMs glued on the G10 frames of different thicknesses.

with an epoxy glue (Figure 3). The anode was segmented in 6×16 mm^2 pads

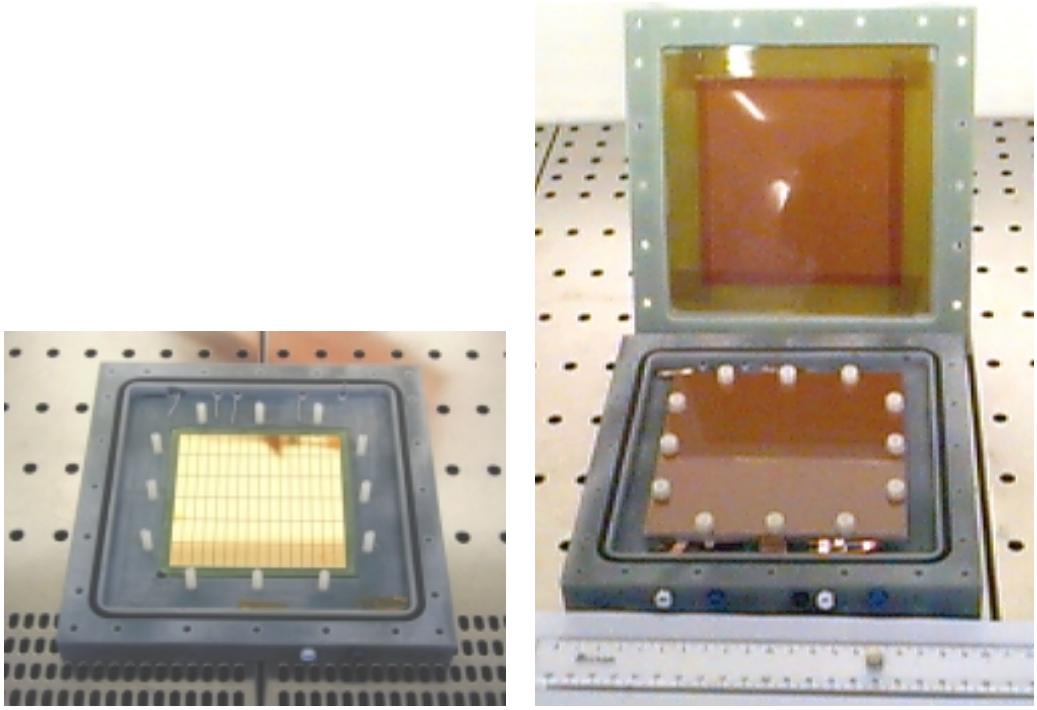

(a) (b)

Fig. 4. (a) Readout pads mounted on the G10 box and (b) the three GEMs stacked in the box. The box acts as both GEM support and gas container.

(Figure 4(a)). The cathode was made of a kapton foil, with copper on one side, glued on a similar frame (Figure 4(b)). All frames were then fixed to the G10 box with nylon screws. The G10 box acted also as gas container.
The high voltage was fed with individual channels to the top and bottom side of each GEM and to the cathode through one 10 MΩ (two 1 MΩ) resistors for detector A (B).
The gas flow rate was set to 2.2 l/h.

5.2 Readout electronics

Fast amplifiers already developed for wire chambers were used. For detector A, 12 pads were equipped with a PNPI design [16] amplifier, already used for tests of prototypes of muon chambers for LHCb; for detector B, 15 pads were equipped with the KLOE-VTX chip [17].
For few pF input capacitance, such as for the pads of our triple-GEM detector, the characteristics of these amplifiers, were quite similar: 5 ns peaking time, 1300 e^- r.m.s. equivalent noise charge, 10 mV/fC sensitivity and 25 Ω (110 Ω) input impedance for detector A (B) for a delta pulse input.

The effective gain G_{eff} of the triple-GEM detector was measured for the two gas mixtures using a high intensity 5.9 KeV X-ray tube.
It was obtained from the relation $G_{eff} = I(eNR)^{-1}$, where I is the measured current on the pads, eN the ionisation charge produced in each conversion (we assumed 200 ionisation electrons per photo-interaction) and R the measured particle rate on the pads with a scaler at the discriminator output. The discriminator threshold for these measurements was set 10 mV higher than the plateu knee for the rate measurement with the $Ar/CO_2/CF_4$ (60/20/20) gas mixture, i.e. 70 mV.
Fig. 5 shows the effective gain as a function of the sum of the voltages applied on the three gem foils with $E_d = 3$ kV/cm and $E_t = 3$ kV/cm.
Our results on the Ar/CO_2 (70/30) gas mixture are in rough agreement

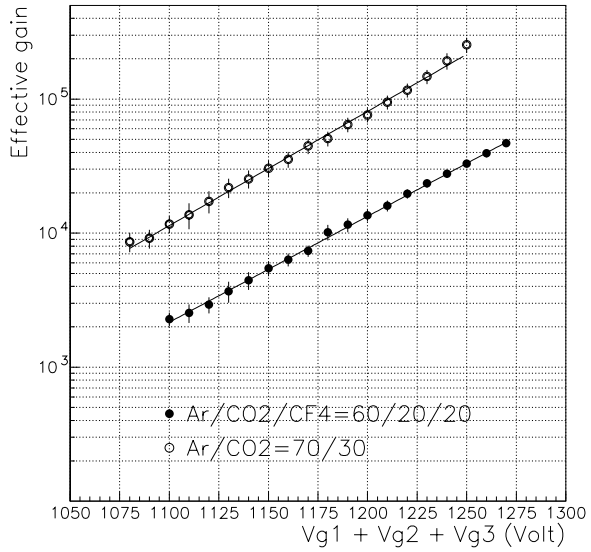

Fig. 5. Effective gain vs. sum of the voltages applied to the three GEM foils, measured with an X-ray tube for the $Ar/CO_2/CF_4$ (60/20/20) and Ar/CO_2 (70/30) gas mixtures with $E_d = 3$ kV/cm and $E_t = 3$ kV/cm.

(within 30 %) with data published by other authors.
It is clear that over the whole range of voltages this measurement spanned, the binary mixture has a larger effective gain by a factor of about five.

5.4 Beam test setup

The measurements were performed at the PS T11 hadron beam facility at CERN. The beam was composed of 2 to 4 GeV pions at a rate of about

1 kHz/cm^2.
The trigger consisted of the coincidence of three scintillators $S1 \otimes S2 \otimes S3$, 10×10 cm^2, 15×15 cm^2 and 1×3 cm^2 respectively, centred on the beam axis, about 1 m from each other. The coincidence of the S1 and S2 signals was sent to a constant fraction discriminator and delayed to give the common stop to a 16-bit multi-hit TDC, with 1 ns resolution and 20 ns double edge resolution. The discriminator threshold on the triple-GEM detector signal was set to about 15 mV, in order to keep the noise count rate below 100Hz.
All signals were sent to a 12 bits charge ADC with 50 fC/count sensitivity.
Detector A (B) was placed 5 cm before (after) S2. The beam was focused near S1 and monitored through a scintillator hodoscope, placed in between S1 and S2, with horizontal and vertical tiles of 1 cm width.
For each run 20,000 triggers were collected.

5.5 Beam test results

For data analysis, events with large ADC signals in the trigger scintillators, which might have originated from two tracks coming within the ADC gate of 200 ns were rejected.
For efficiency measurement, the time of the event was defined as the first time of threshold crossing among those channels which were above threshold.
The two chambers showed very similar performances in terms of efficiency and pad multiplicity. Therefore, in the following no mention to chamber type will be given anymore.
In our detectors no discharges with current exceeding 2 μA in 0.1 s and no current was observed with the HV power supply sensitivity of 100 nA. However, a detailed study of discharge rate was not performed.

5.5.1 Efficiency

Figure 6(a) and Figure 6(b) show the time distributions obtained with the Ar/CO_2 and $Ar/CO_2/CF_4$ gas mixtures, respectively, for U_{gem2} =U_{gem3} = 390 V, U_{gem1} = 450 V, E_d = 3 kV/cm and E_t = 3 kV/cm (E_t = 4 kV/cm for figure 6(b)).
The zero of the time scale is at a fixed delay after the trigger (includes cable delays etc.).
The two figures show a clear asymmetry with a marked tail towards large times.

This tail is also correlated with signal amplitude, as shown in Figure 7 for the run with the $Ar/CO_2/CF_4$ gas mixture.
We understand this tail and its correlation with signal amplitude as coming

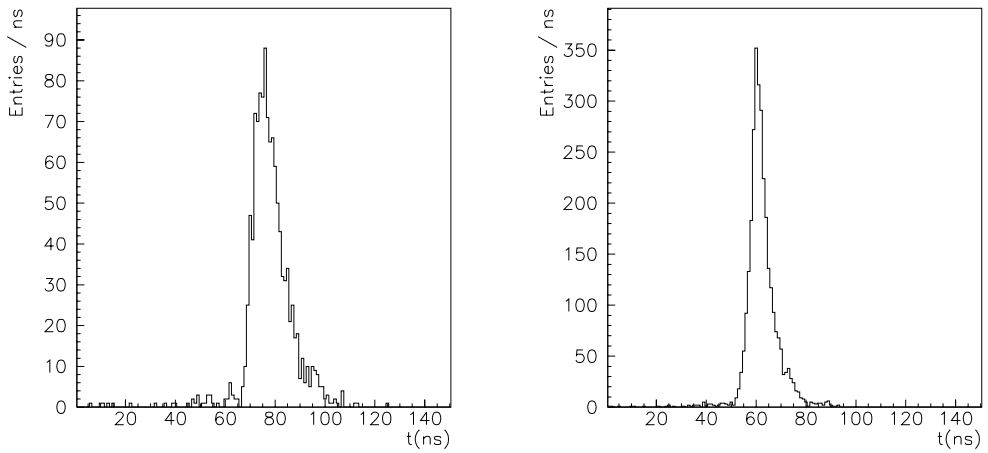

(a) (b)

Fig. 6. Time distributions with Ar/CO_2 (70/30) (a) and $Ar/CO_2/CF_4$ (60/20/20) (b). The r.m.s. of the two distributions are 9.7 and 5.9 ns, respectively.

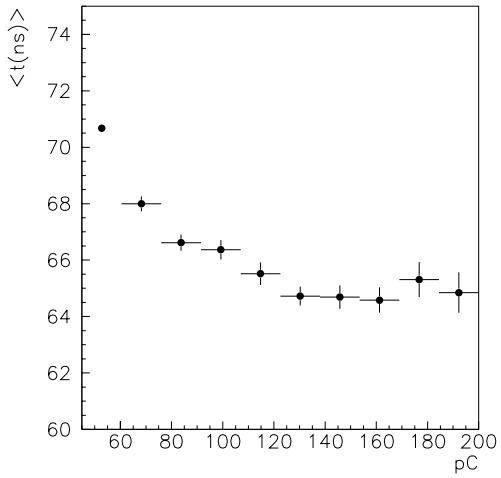

Fig. 7. Time vs. signal amplitude, as measured by the charge ADC, with the $Ar/CO_2/CF_4$ gas mixture.

from the statistics of primary cluster production, as discussed in section 4.
The entries at early times can be explained by the *bi-GEM effect*, mentioned in section 4 and they amount to 1 to 2% of the total number of entries, depending on GEM voltage values.
The r.m.s. of the distribution in Figure 6(a) is 9.7 ns. For comparison, a measurement by other authors [4], obtained with a bi-GEM detector and a four times slower rise-time amplifier, gave a Gaussian fit σ of 9.9 ns without software corrections.
The r.m.s. of the distribution in Figure 6(b) is 5.9 ns, i.e. 40% narrower than

that of the binary mixture. The smaller improvement in time resolution observed in the data compared to expectations of section 4 can be explained by the different gain measured with the two mixtures (see section 5.3).
The different mean value of the time distributions with the two gas mixtures is also in rough agreement with the difference in the drift velocity, taking also into account the drift of electrons in the two transfer gaps (E_t was different for the runs corresponding to the two Figures).

Effect of the drift field

The plot in Figure 8(a) shows, for the $Ar/CO_2/CF_4$ gas mixture, the efficiency measured in a 300 ns (which we call global efficiency) and 25 ns time window as a function of the drift field E_d, when E_{t1} =E_{t2} = 4 kV/cm and U_{gem1} =U_{gem2} =U_{gem3} = 375 V. For E_d = 3 kV/cm a global efficiency of a 96% is reached, decreasing to 87% for 25 ns. The plot displays an optimum value, at about 3 kV/cm. At low field values, the efficiency loss can be explained by the low drift velocity and, at high fields, by the defocusing effect of field lines above the GEM bringing the ionisation electrons to directly impinge on the upper copper layer. This last effect was also observed by the authors of [14], who measured the absolute transfer efficiency of GEMs with the Ar/CO_2 (70/30) gas mixture.
A similar behaviour was observed for the other gas mixture.

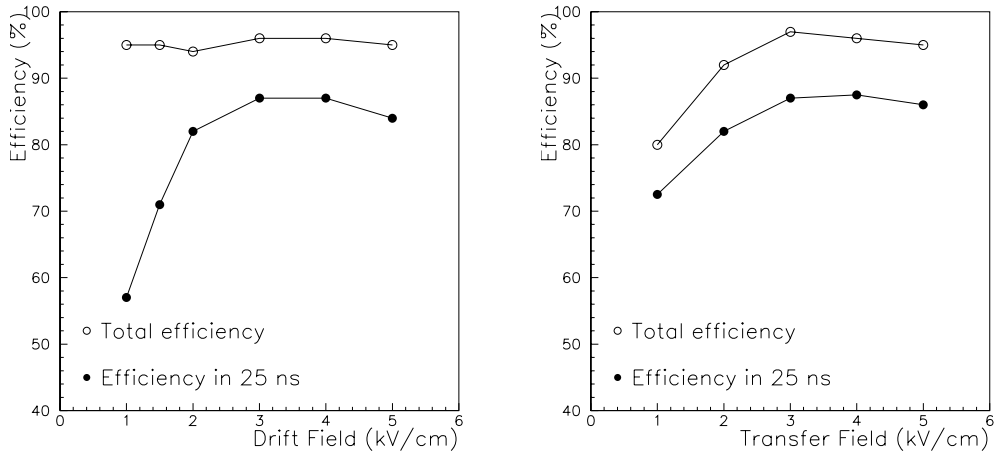

(a) (b)

Fig. 8. Detection efficiency as a function of (a) the drift field and of (b) the transfer field, with E_{t1} =E_{t2}, for the $Ar/CO_2/CF_4$ mixture.

Effect of the transfer field

The efficiencies are shown in Figure 8(b) as a function of the transfer field value, with $E_d = 3$ kV/cm and $U_{gem1} = U_{gem2} = U_{gem3} = 375$ V.
The plot shows an optimum value at about 3 kV/cm, where the efficiencies are 97 % and 87 % for the 300 ns and the 25 ns time window, respectively.
At small transfer field we observed an efficiency loss, which can be explained by a poorer electron extraction capability from the lower side of the GEM. At high transfer field the efficiency drops. This can be explained by a smaller collection efficiency from the second GEM and third GEM.
A similar behaviour is observed for the other gas mixture.

Effect of voltage on the first GEM

The efficiencies for the various time windows as function of U_{gem1} are shown in Figure 9(a) (b)) for the Ar/CO_2 ($Ar/CO_2/CF_4$) gas mixture, for E_d = 3 kV/cm, U_{gem2} =U_{gem3} = 390 V, $E_t = 4$ kV/cm. Efficiencies of 90 % (85 %) in 25 ns (20 ns) window were obtained at the highest value of U_{gem1} with Ar/CO_2 while of 96% (93%) in a 25 ns (20 ns) window with $Ar/CO_2/CF_4$, confirming the better timing properties of the ternary gas mixture. It should be noticed that the comparison is made at equal voltage; were it made at equal gain, the ternary mixture would have had even better timing properties.
The choice of increasing the gain of the first GEM rather than of all three

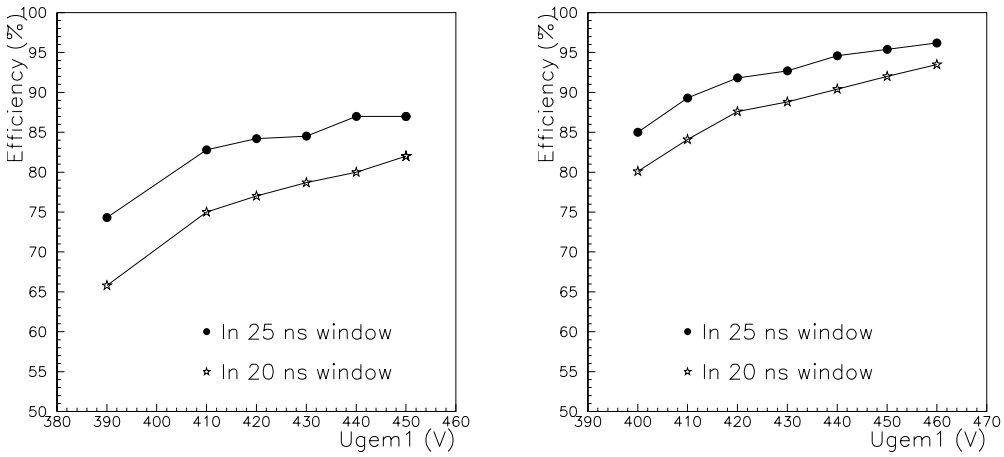

(a) (b)

Fig. 9. Detector efficiencies as a function of U_{gem1} with Ar/CO_2 (a) and $Ar/CO_2/CF_4$ (b).

GEMs altogether to improve the time performance, as discussed in section 4, finds also some justification from the data. Two runs, with the Ar/CO_2 mix-

ture, were taken with different voltage configurations on the three GEMs but with equal voltage sum: run i) with U_{gem1} = 410 V, U_{gem2} = 390 V and U_{gem3} = 390 V and run ii) with U_{gem1} = 390 V, U_{gem2} = 400 V and U_{gem3} = 400 V. The measured average charges are, as expected, equal within few %. However, run i) has a 50% smaller *bi-gem* event fraction and the r.m.s. of the distribution 11 % narrower.
It should be noticed that the efficiency plots as a function of various parameters display a smooth behaviour. This is a good indication for stability in long time operation of the detector.

5.5.2 Pad multiplicity

The pad dimension used in this test was 6×16 mm^2, i.e. smaller than needed for LHCb operation.
The obtained pad multiplicity at U_{gem1}=460 V is, for the Ar/CO_2 ($Ar/CO_2/CF_4$) gas mixture, 1.6 (1.5). Since the discriminator threshold was kept fixed during the whole beam test, the pad multiplicity increased with signal amplitude. For example, it increased by 17% when U_{gem1} went from 400 V to 460 V.
As a rough estimate of multiplicity with larger pads, it was possible in the offline analysis to add three pads together, obtaining a *software pad* of size 18×16 mm^2. The pad multiplicity so obtained was 1.1 for both mixtures.
Our result on pad multiplicity is clearly worse than what would naively expect from published data. However, it is fair to say that a thorough comparison is difficult since cross-talk strongly depends on details of front-end circuitry such as input impedance and shaping functions and threshold values. A detailed study of this issue will be the subject of future studies.

6 Conclusions

A time performance study of triple-GEM detectors was performed both with simulation and beam test measurements, through a detailed investigation of the role played by detector geometry, electric fields and gas mixture.
With the ternary gas mixture $Ar/CO_2/CF_4$ (60/20/20) we obtained a time distribution r.m.s. without software corrections of about 6 ns and an efficiency of 96 % (93 %) in a 25 ns (20 ns) time window, considerably improving results obtained in the past with the Ar/CO_2 (70/30) mixture.
These results make the triple-GEM detector a promising option for high rate charged particle triggering at LHC.
High rate, ageing performance and discharge probability measurement with the optimised detector configuration will be the subject of a future publication.

7 Acknowledgements

The authors would like to thank F. Sauli for useful discussions. This work would not have been possible without the support of the technical staff both at INFN Cagliari and at LNF, and in particular of: M. Arba and M. Tuveri (INFN Cagliari) for the realization of the mechanics of the Cagliari prototype; D. Marras (INFN Cagliari) for the design and the assembly of the front-end electronics of the Cagliari prototype; B. Ortenzi (LNF) for the design of the detector box of the Frascati prototypes; E. Iacuessa and S. Valeri for the realization of the mechanics of the Frascati prototypes; the LNF Electronics Pool for the realization of the front-end electronics of the Frascati prototypes.

References

[1] F. Sauli, Nucl. Instrum. Meth. **A386**, 531 (1997).

[2] S. Bachmann et al., CERN-EP/2000-116, 31 August 2000.

[3] T.Zeuner,Nucl. Instrum. Meth. **A446**, 324 (2000)

[4] A. Bressan et al., Nucl. Instrum. Meth. **A425**, 262 (1999).

[5] LHCb Muon System Technical Design Report, CERN LHCC 2001-010, LHCb TDR 4, (2001).

[6] S. Bachmann et al., CERN-EP/2000-151, 11 December 2000.

[7] H.R.Schmidt et al, ALICE note 1999-56.

[8] F.Sauli, CERN Report 77-09 (1977).

[9] S. Bachmann et al., Nucl. Instrum. Meth. **A438**, 376 (1999).

[10] U. Becker et al., "Gas R&D Home Page (http://cyclotron.mit.edu/drift)".

[11] I.Smirnov, HEED, program to compute energy loss of fast particles in gas, Version 1.01, CERN.

[12] MAXWELL 3d extractor, ANSOFT.

[13] R.Veenhof, GARFIELD, a drift chamber simulation program, Version 7.02, CERN.

[14] C.Richter et al., Nucl. Instrum. Meth. **A461**, 38 (2001).

[15] A. Gandi, Laboratory of Photomechanical Techniques and Printed Circuits, EST-SM-CI Section, CERN, Geneva, Switzerland.

[16] A.Vorobyov et al, LHCb note 2000-003.

[17] R.J. Yarema et al.,IEEE Trans. Nucl. Sci.,**39**, No. 4, 742(1992)